Since January 2020 Elsevier has created a COVID-19 resource centre with free information in English and Mandarin on the novel coronavirus COVID-19. The COVID-19 resource centre is hosted on Elsevier Connect, the company's public news and information website.

Virology 388 (2009) 112–120

Contents lists available at ScienceDirect

Virology

journal homepage: www.elsevier.com/locate/yviro

APOBEC3G cytidine deaminase association with coronavirus nucleocapsid protein

Shui-Mei Wang, Chin-Tien Wang *

Department of Medical Research and Education, Taipei Veterans General Hospital, 201, Sec. 2, Shih-Pai Road, Taipei 11217, Taiwan
Institute of Clinical Medicine, National Yang-Ming University, Taipei, Taiwan

ARTICLE INFO

Article history:
Received 2 December 2008
Returned to author for revision
9 January 2009
Accepted 10 March 2009
Available online 5 April 2009

Keywords:
APOBEC3G
Coronavirus
SARS-CoV
HCoV-229E
HIV-1
Nucleocapsid

ABSTRACT

We previously reported that replacing HIV-1 nucleocapsid (NC) domain with SARS-CoV nucleocapsid (N) residues 2–213, 215–421, or 234–421 results in efficient virus-like particle (VLP) production at a level comparable to that of wild-type HIV-1. In this study we demonstrate that these chimeras are capable of packaging large amounts of human APOBEC3G (hA3G), and that an HIV-1 Gag chimera containing the carboxyl-terminal half of human coronavirus 229E (HCoV-229E) N as a substitute for NC is capable of directing VLP assembly and efficiently packaging hA3G. When co-expressed with SARS-CoV N and M (membrane) proteins, hA3G was efficiently incorporated into SARS-CoV VLPs. Data from GST pull-down assays suggest that the N sequence involved in N–hA3G interactions is located between residues 86 and 302. Like HIV-1 NC, the SARS-CoV or HCoV-229E N-associated with hA3G depends on the presence of RNA, with the first linker region essential for hA3G packaging into both HIV-1 and SARS-CoV VLPs. The results raise the possibility that hA3G is capable of associating with different species of viral structural proteins through a potentially common, RNA-mediated mechanism.

Introduction

Apolipoprotein B mRNA-editing enzyme-catalytic polypeptide-like 3G (APOBEC3G) is a member of the APOBEC3 family of cytidine deaminases (Cullen, 2006). Human APOBEC3G (hA3G) can be packaged into HIV-1 virions to mediate C-to-U editing on nascent proviral minus strands during reverse transcription, resulting in the inhibition of viral replication (Harris et al., 2003; Mangeat et al., 2003; Yu et al., 2004; Zhang et al., 2003). Accordingly, hA3G as an anti-viral factor confers innate immunity to HIV-1. However, HIV-1 encodes Vif, which counteracts hA3G by inducing hA3G degradation via the ubiquitin–proteasome pathway, thereby blocking its incorporation into budding virions (Mehle et al., 2004; Yu et al., 2003). The ability of Vif to negate hA3G function is both dependent on physical association and partly species-specific—in other words, Vif cannot counteract a form of A3G from a different species. This inefficient Vif–hA3G interaction means that HIV-1 Vif is capable of counteracting human and chimpanzee A3G, but not mouse A3G (mA3G) or African green monkey A3G (Mariani et al., 2003). Other researchers have shown that hA3G or other APOBEC family members can confer innate immunity to a wide range of retroviruses as well as HBV (which is similar to retroviruses in that it also goes through a reverse transcription step during genomic replication) (Cullen, 2006).

The incorporation of A3G into HIV-1 virions is mediated by the Gag nucleocapsid (NC) domain (Alce and Popik, 2004; Cen et al., 2004; Khan et al., 2005; Luo et al., 2004; Schafer et al., 2004; Zennou et al., 2004). In addition to playing a key role in viral RNA packaging (Berkowitz et al., 1993, 1995; Poon et al., 1996; Zhang and Barklis, 1997), NC contains an I domain that is responsible for Gag–Gag interactions (Bennett et al., 1993; Bowzard et al., 1998). Heterologous polypeptides capable of self-association have been shown to confer the ability to efficiently produce chimeric VLPs when substituted for HIV-1 NC (Accola et al., 2000; Burniston et al., 1999; Johnson et al., 2002; Zhang et al., 1998). However, replacing NC with a leucine-zipper motif that does not encapsidate RNA abolishes hA3G packaging without significantly affecting HIV-1 virion production (Zennou et al., 2004), suggesting RNA involvement in hA3G incorporation. This is consistent with the proposal that RNA is required for either hA3G viral incorporation or Gag–hA3G interaction (Khan et al., 2005; Schafer et al., 2004; Svarovskaia et al., 2004; Zennou et al., 2004). We previously demonstrated that HIV-1 Gag mutants containing severe acute respiratory syndrome coronavirus nucleocapsid (SARS-CoV N) coding sequences as NC substitutes can effectively assemble VLPs (Wang et al., 2008). While completely unrelated, the SARS-CoV N protein is similar to HIV-1 NC in that it contains putative protein–protein interaction domains (He et al., 2004; Narayanan et al., 2003; Surjit et al., 2004; Yu et al., 2005) and plays a role in viral RNA packaging (Hsieh et al., 2005; Huang et al., 2004a).

Given that SARS-CoV N possesses a RNA-binding property, it is likely that assembly-competent chimeras containing a replacement of HIV-1 NC by an SARS-CoV N sequence may support the incorporation of hA3G into VLPs. Here we demonstrate that the

* Corresponding author. Fax: +886 2 28742279.
E-mail address: chintien@ym.edu.tw (C.-T. Wang).

0042-6822/$ – see front matter © 2009 Elsevier Inc. All rights reserved.
doi:10.1016/j.virol.2009.03.010

carboxyl-terminal half of the SARS-CoV or human coronavirus 229E (HCoV-229E) N protein not only enables efficient VLP production, but also confers the ability to efficiently package human APOBEC3G (hA3G) when substituted for HIV-1 NC. Direct evidence comes in the form of hA3G being efficiently packaged into SARS-CoV VLPs. The interaction between coronavirus N and hA3G is also RNA-dependent. This implies that in addition to retroviruses, SARS-CoV and other RNA viruses may be capable of packaging hA3G via nucleocapsid domains.

Results

Interaction between SARS-CoV nucleocapsid protein and human APOBEC3G

We previously reported that the HIV-1 Gag chimeras containing the SARS-CoV N carboxyl-terminal 215–421 [NC(N2)] or 234–421 [NC(N4)] codons in the deleted NC region (Fig. 1) are capable of assembling VLPs as efficiently as wt Gag (Wang et al., 2008). This raises the question of whether the inserted SARS-CoV N sequence confers the chimeric ability to package hA3G. We therefore co-expressed assembly-competent NC(N2) and NC(N4) with hA3G in 293T cells and used Western immunoblotting to detect VLP-associated hA3G. Our controls were the HIV-1 NC-deleted mutants ΔNC, ΔPC, and delNC, all with different numbers of deleted NC codons (Fig. 1). Our results show that NC(N2) and NC(N4) were capable of packaging hA3G at the same efficiency level as the wild-type (Fig. 2A, lanes 6 and 7 vs. lane 2). Low but detectable VLP-associated hA3G was observed in the NC-deletion mutants (lanes 4 and 5). Since HIV-1 Vif inhibits hA3G virion incorporation by triggering hA3G degradation (Conticello et al., 2003; Kao et al., 2003; Liu et al., 2004; Mariani et al., 2003; Marin et al., 2003; Mehle et al., 2004; Sheehy et al., 2003; Stopak et al., 2003; Yu et al., 2003), the hA3G expression level or the presence of Vif may affect the level of virus-associated hA3G. To test whether Vif or hA3G expression level affects hA3G packaging into chimeric VLPs, we introduced mutation-blocking Vif expression into wt and NC(N2) and co-transfected each Vif-deficient (ΔVif) result with different amounts of the hA3G-coding plasmid. In the absence of Vif, we observed a relatively higher steady-state hA3G expression level accompanied by an increased level of VLP-associated hA3G (Fig. 2B, right top panel). Members of the ΔVif group occasionally expressed higher VLP levels than their Vif-intact counterparts (Fig. 2B, lanes 6–9 vs. 2–5). However, we also repeatedly observed ΔVif group members producing higher levels of VLP-associated hA3G. In the presence or absence of Vif, NC(N2) displayed a level of VLP-associated hA3G comparable to that displayed by wt. These results suggest that the SARS-CoV N carboxyl-terminal region can be substituted for HIV-1 NC without affecting VLP assembly or hA3G packaging functions.

To determine the required SARS-CoV N sequences for conferring hA3G packaging ability, we co-expressed hA3G with wt or with chimeras containing a variety of N coding regions as HIV-1 NC substitutes. As illustrated in Fig. 1, full-length SARS-CoV N sequences were inserted into the ΔNC (ΔNC[CoN]) and delNC (NC[CoN]) constructs. NC(N1), NC(N3), NC(N5), NC(N6), and NC(N7) respectively contain N codons 2–213, 215–359, 302–421, 2–168, and 2–86 in the deleted NC region. We again found that both NC(N2) and NC(N4) were capable of efficiently packaging hA3G at VLP-associated hA3G levels comparable to or higher than those of wt (Fig. 2C, lanes 5 and 7). Even though ΔNC(CoN) and NC(CoN) were found to be defective in VLP production, they incorporated hA3G at an efficiency level comparable to that of wt (lanes 2 and 3). Further, despite producing substantial amounts of VLPs, the NC(N1) was incapable of packaging hA3G as efficiently as wt (i.e., it produced a VLP-associated hA3G level approximately 60% that of wt) (lane 4). The barely detectable level of VLP-associated hA3G found in NC(N6) may be due to lower levels of VLPs in the blot and/or lower levels of hA3G expression (Fig. 2C). However, in a separate blot containing higher VLP and hA3G expression levels, VLP-associated hA3G in NC(N6) was approximately 50% that measured in wt (data not shown).

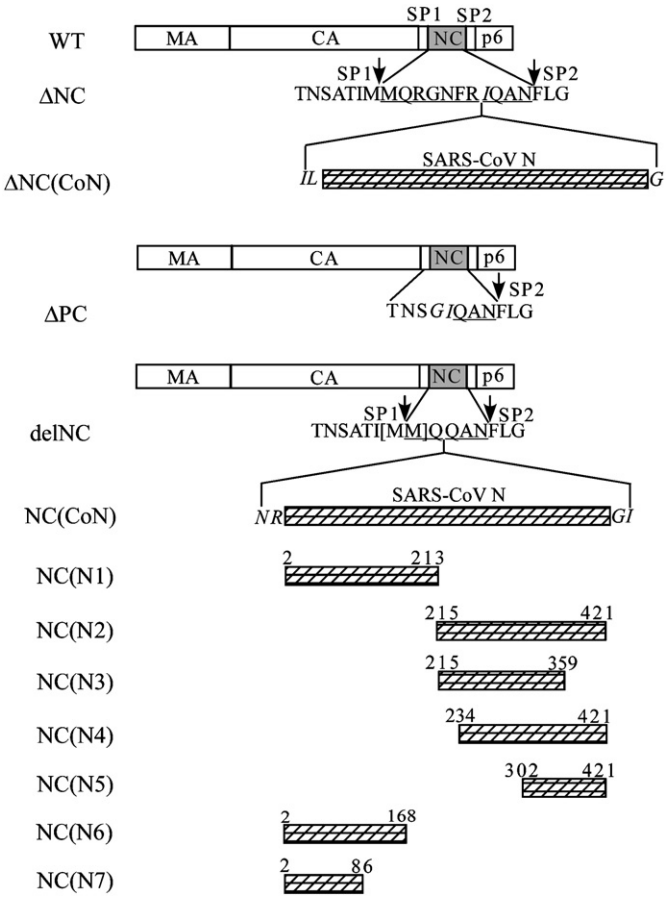

Fig. 1. Schematic representation of chimeric constructs. Shown are mature HIV-1 Gag protein domain matrix (MA), capsid (CA), nucleocapsid (NC), p6, and amino acid residues in SP1-NC-SP2 junction. ΔNC has ten HIV-1 NC residues remaining in the deleted region; ΔPC has NC almost deleted, with SP1 partially removed. delNC has the two methionine residues (bracketed) in the SP1-NC junction removed. PCR-amplified fragments containing various portions of SARS-CoV N coding sequences were inserted into the deleted NC regions. Numbers denote codon positions at inserted SARS-CoV N protein sequence boundaries. Arrows indicate SP1-NC and NC-SP2 junction sites. Remaining HIV-1 NC residues in deleted regions are underlined. Altered or foreign amino acid residues inserted in juncture area are italicized. All constructs were expressed in HIVgptD25 (a HIV-1 PR-defective expression vector).

Both hA3G viral incorporation and Gag–hA3G interaction require the presence of RNA (Khan et al., 2005; Schafer et al., 2004; Svarovskaia et al., 2004; Zennou et al., 2004). We tested whether the association between SARS-CoV N and hA3G has the same requirement by fusing the SARS-CoV N amino-terminal (N1, N6, and N7) or carboxyl-terminal sequence (N2, and N5) to the carboxyl terminus of GST and co-expressing each GST fusion construct with hA3G. Cell lysates containing hA3G and GST fusions were treated with RNase prior to performing a GST pull-down assay. Results indicate that GST-CoN, GST-N1, GST-N2, and GST-N6 were capable of pulling down hA3G, whereas the amount of hA3G associated with GST fusion was markedly reduced following RNase treatment (Fig. 3). Neither GST-N5 nor GST-N7 was capable of pulling down hA3G, regardless of whether or not they were treated with RNase (Fig. 3, lanes 7, 9, 16 and 18). These results suggest that (a) the hA3G-binding domain of SARS-CoV N is largely contained within the sequence between residues 86 and 302, and (b) efficient N–hA3G interactions occur in a RNA-dependent manner.

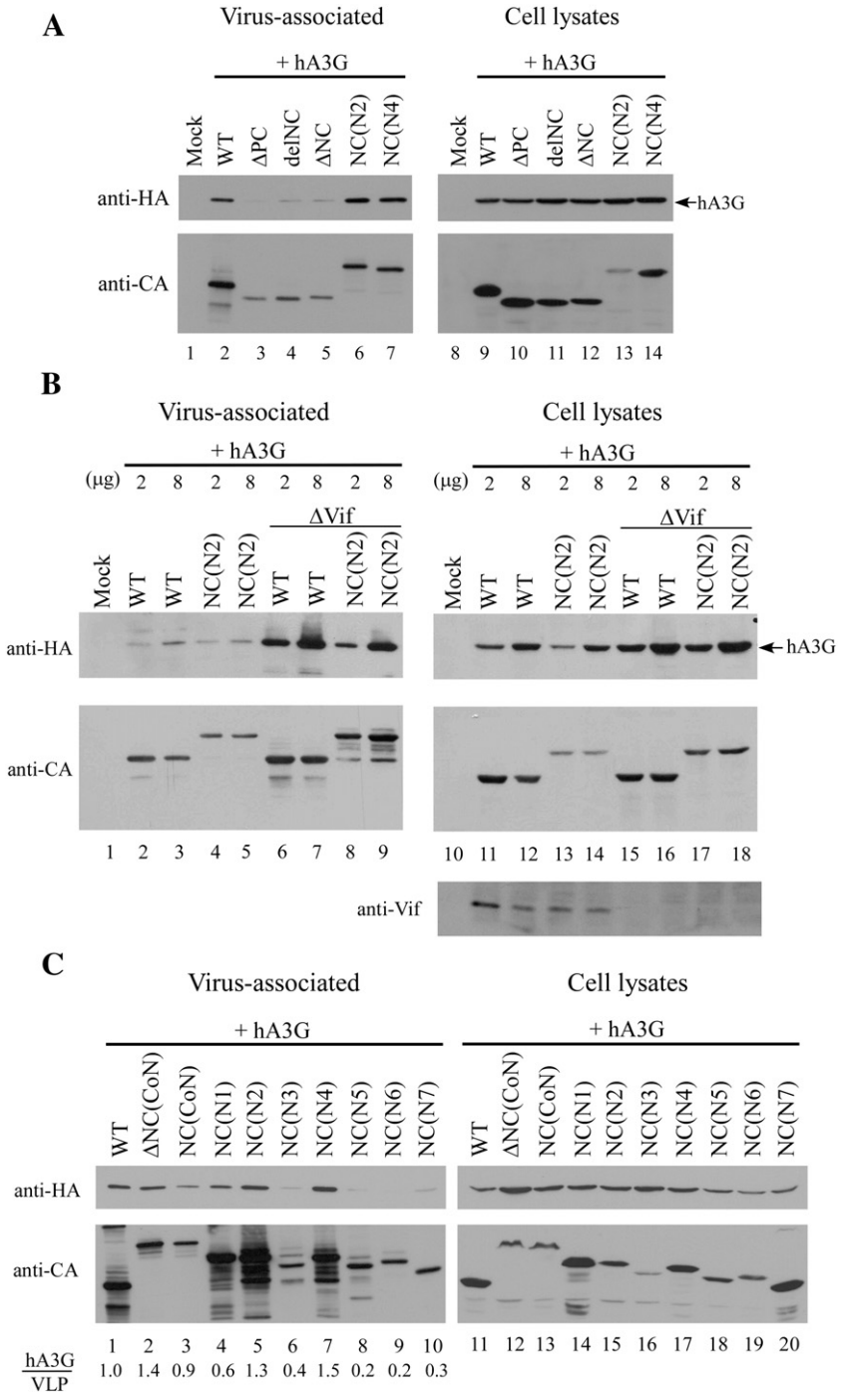

Fig. 2. Incorporation of human APOBEC3G into VLPs. 293T cells were co-transfected with a human APOBEC3G (hA3G) expression vector and indicated plasmid. At 48–72 h post-transfection, cells and supernatant were collected and subjected to Western immunoblotting. hA3G plasmid DNA (2 or 8 μg) was used for co-transfection as indicated. ΔVif is a Vif-deficient mutation introduced into wt and NC(N2) (panel B, lanes 6–9). Wild-type Gag and chimeric proteins were probed with a monoclonal antibody directed against HIV-1 CA; an anti-HA monoclonal antibody was used to detect hA3G. Vif antiserum was used to detect Vif. Relative levels of VLP-associated hA3G are indicated along the bottom (panel C). hA3G, wt Gag, and chimeric proteins were quantified by scanning hA3G and p24CA-associated band densities from immunoblots. Ratios of hA3G to $p24^{gag}$ were determined and normalized to that of wt.

Incorporation of human APOBEC3G into SARS-CoV virus-like particles

To test whether hA3G can be efficiently packaged into SARS-CoV, we transfected 293T cells containing the hA3G-coding plasmid with SARS-CoV M and N expression vectors. SARS-CoV VLPs were generated by co-expressing M and N proteins (Huang et al., 2004b). Results indicate that the amount of SARS-CoV VLP-associated hA3G was comparable to that of HIV-1 (Fig. 4A, lane 4 vs. lane 5). Medium hA3G was not detected when co-expressed with M or N alone. Extracellular N was also undetectable without M co-expression (data not shown). Results from co-immunoprecipitation experiments indicate that N was capable of associating with hA3G but M was not (data not shown). The data suggest that hA3G packaging into SARS-CoV VLPs largely depends on hA3G–N association.

To further confirm an association between released hA3G and SARS-CoV VLPs formed by M and N, supernatant pellets derived from

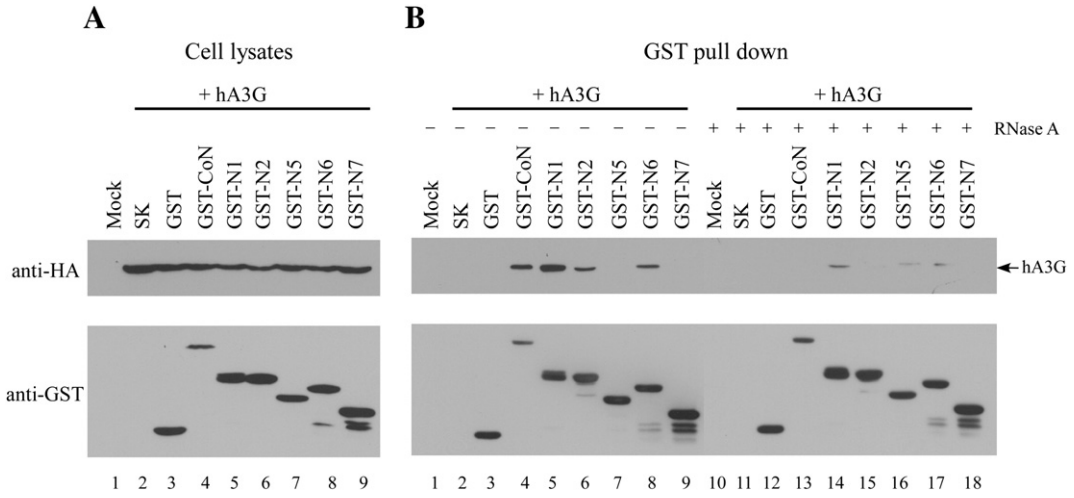

Fig. 3. RNase A treatment significantly affected SARS-CoV N association with human APOBEC3G. (A) 293T cells were co-transfected with a human A3G (hA3G) expression vector and pBlueScript SK or indicated GST fusion construct. Cell lysates were subjected to Western immunoblotting 48 h post-transfection. (B). Equal amounts of cell lysates were treated with (lanes 10–18) or without (lanes 1–9) 0.2 mg/ml DNase-free RNase A for 30 min at 25 °C, followed by mixing with glutathione-agarose beads for 2 h at 4 °C. Complexes bound to the beads were pelleted, washed, and subjected to Western immunoblotting with anti-HA and anti-GST antibodies.

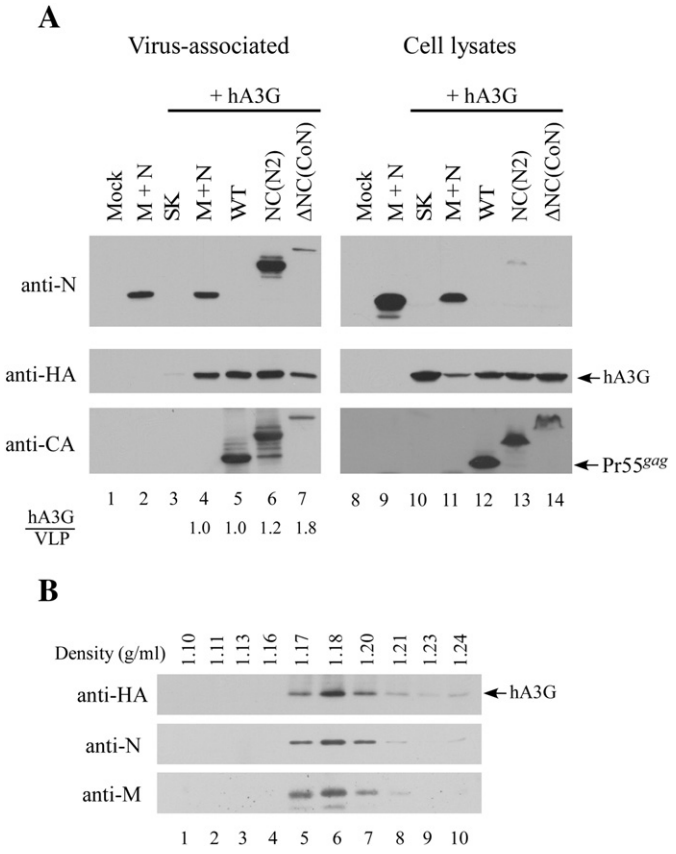

Fig. 4. Incorporation of human APOBEC3G into SARS-CoV VLPs. (A) 293T cells were transfected with hA3G expression vector alone or together with plasmids encoding SARS-CoV M (membrane) and N, or with the indicated plasmids. At 48–72 h post-transfection, supernatant and cells were harvested, prepared, and subjected to Western immunoblotting. Levels of p24CA-, N-associated proteins and virus-associated hA3G in each sample were quantified by scanning immunoblot band densities. Ratios of VLP-associated hA3G versus p24CA-associated or N-associated protein levels were calculated for each sample and normalized to that of hA3G associated with wt VLPs in parallel experiments. (B) Sucrose density gradient fractionation analysis of SARS-CoV VLPs. 293T cells were co-transfected with hA3G, M and N expression vectors. At 48–72 h post-transfection, supernatants were collected and pelleted through 20% sucrose cushions. Viral pellets were resuspended in PBS buffer and centrifuged through a 20 to 60% sucrose gradient for 16 h. Fractions were collected from top to bottom, measured for density and analyzed for hA3G, M, and N proteins level by immunodetection. Densities of each fraction are indicated on the top.

cells co-transfected with hA3G, M, and N expression vectors were subjected to sucrose density gradient fractionation experiments. The results shown in Fig. 4B indicate that both M and N had fraction 6 peaks at a density of 1.18 g/ml, which is consistent with a previous report on SARS-CoV virus-like particle density (Huang et al., 2004b). A hA3G peak was also found at fraction 6, suggesting an association between hA3G and SARS-CoV VLPs generated via M and N co-expression.

Mapping the SARS-CoV N-binding domain of human APOBEC3G

Members of the APOBEC3 protein family share a highly conserved zinc-coordinating motif: His-X-Glu-X_{23-28}-Pro-Cys-X_{2-4}-Cys (Chen et al., 2007b). Similar to APOBEC1, APOBEC3G contains two zinc-coordinating motifs, with the carboxyl-terminal zinc-coordinating motif possessing catalytic cytidine deaminase activity. To identify hA3G regions responsible for hA3G incorporation into SARS-CoV VLPs, we co-transfected 293T cells with M and N expression vectors and a plasmid encoding wt or a hA3G mutant containing various carboxyl- or amino-terminus deletions (Fig. 5A). The results indicate that hA3G mutants lacking residues 1–104, 157–384, or 246–384 were capable of being incorporated into VLPs, and that hA3G mutants lacking residues 1–156 or 309–384 were undetectable in the medium samples (Fig. 5B, lanes 4 and 7). In the cases of Δ246–384 and Δ309–384, poor particle incorporation may be due in part to low expression levels. In particular, Δ309–384 was barely detectable in repeat experiments. Low steady-state expression levels of the carboxyl-terminal truncated hA3G mutant have been reported previously (Cen et al., 2004). In comparison, the Δ157–384 mutant expressed greater steady-state stability and a higher level of VLP-associated hA3G (lanes 5 and 12). To test whether the mutations had similar effects on hA3G packaging into chimeric VLPs, wt or each hA3G mutant was individually co-expressed with NC(NC2) (which contains the carboxyl-terminal half of the N coding sequence and is known to efficiently produce VLPs and package hA3G) (Figs. 1 and 2). Our results indicate that the hA3G mutations exerted similar effects on hA3G packaging into NC(N2) VLPs with no detectable VLP-associated Δ1–156 or Δ309–384 (Fig. 5C).

Combined, these results suggest that the essential region for hA3G packaging into SARS-CoV VLPs is located between residues 104 and 156, corresponding to the first linker region. To test whether the deletion mutations exerted similar effects on hA3G incorporation into HIV-1 VLPs, we co-expressed wt or each hA3G deletion mutant

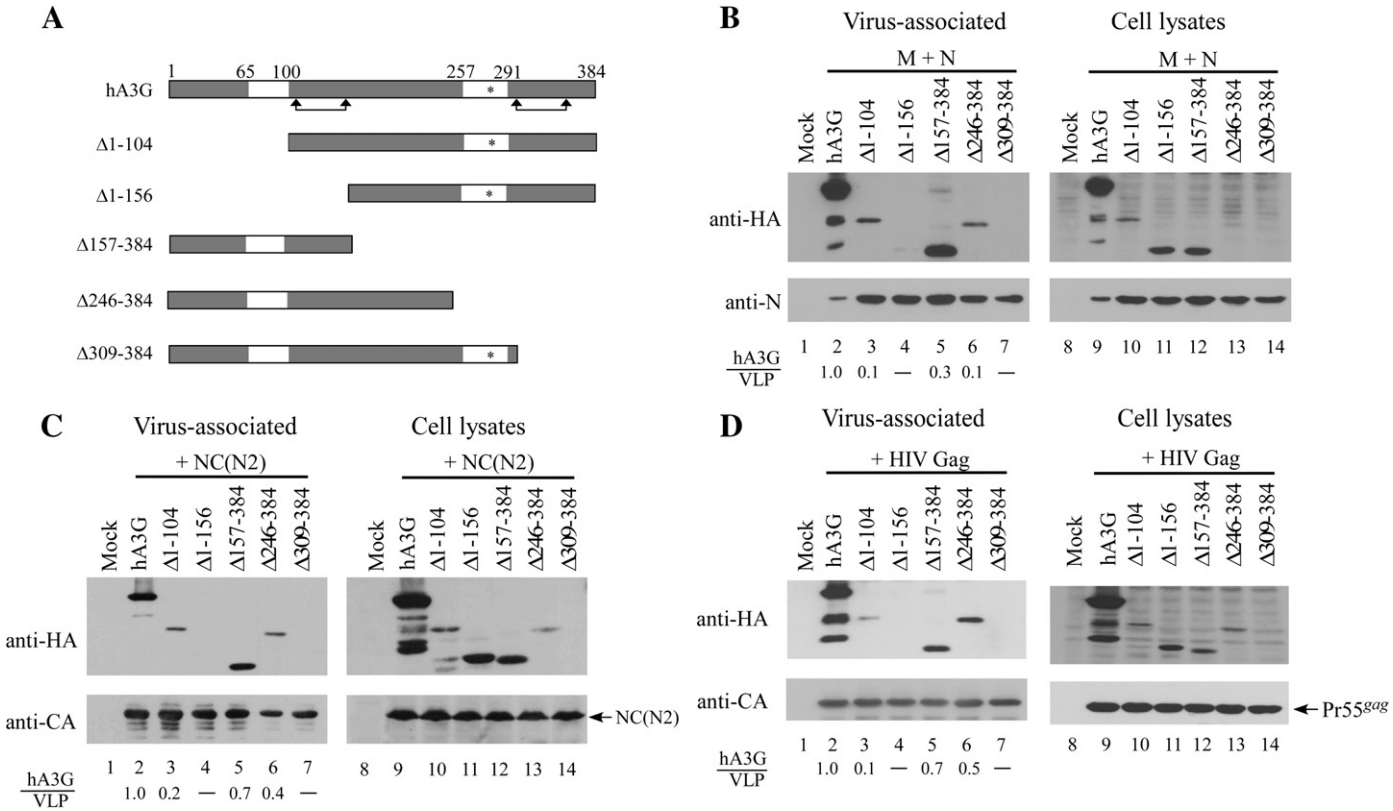

Fig. 5. Incorporation of human APOBEC3G into VLPs. (A) Schematic representatives of wt and human APOBEC3G (hA3G) expression constructs. Open boxes indicate the zinc-coordinating motif, HXE-X_{23-28}-$CX_{2-4}C$. The asterisk denotes the cytidine deaminase catalytic site. Domains that previously referred to the "linker" peptides are depicted by arrowheads. Numbers denote amino acid positions in hA3G. Indicated positions of deleted hA3G amino acid residue boundaries were used to designate mutant hA3G constructs. Note that each hA3G deletion mutant was tagged with a single copy of HA at the carboxyl terminus and that the wt hA3G was triple-tagged with HA. This may have caused a higher signal for the detected wt hA3G, thus leading to underestimates of the VLP-associated hA3G deletion mutants. (B–D) Incorporation of wt and mutant hA3G into VLPs. 293T cells were co-transfected with M and N, NC(N2) or an HIV-1 Gag expression vector (HIVgptD25) plus each of the hA3G expression vectors. To avoid effects from Vif on hA3G expression level, NC(N2) and HIVgptD25 were expressed in Vif-deficient (ΔVif) contexts. At 48–72 h post-transfection, supernatant and cells were harvested, prepared, and subjected to Western immunoblotting. M and N were probed with M antiserum and an anti-N monoclonal antibody. hA3G was probed with an anti-HA antibody and wt Gag and chimeric proteins were detected with an anti-p24CA antibody. Levels of p24CA- and N-associated proteins and virus-associated hA3G in each sample were quantified by scanning immunoblot band densities. Ratios of total hA3G versus p24CA-associated or N-associated protein levels were calculated for each sample and normalized to that of wt hA3G in parallel experiments. Dashes (–) denote ratios below 0.01. Similar results were observed in repeat and independent experiments. The immunoblots presented here were intentionally overexposed to allow for visualization of the individual hA3G mutants.

individually with HIV-1 Gag. In agreement with previous reports (Cen et al., 2004; Luo et al., 2004), the Δ1–156 mutation (with a deletion involving the first linker region) blocked hA3G incorporation (Fig. 5D, lane 4). Overall, the deletion mutations had similar effects on hA3G packaging into HIV-1, NC(N2), and SARS-CoV VLPs. Specifically, the essential domain for incorporating hA3G into HIV-1 and SARS-CoV VLPs was located in the same (first) linker region.

Association between human coronavirus 229E nucleocapsid protein and hA3G

To test whether the SARS-CoV N ability to confer hA3G packaging is dependent on N–hA3G interaction and therefore distinct from its self-interaction capacity, we co-expressed hA3G with an assembly-competent Gag containing a leucine-zipper domain as a NC substitute. Inserting a wild-type leucine-zipper (wtZiP) domain into the deleted NC region restored VLP production to wt level (Fig. 6A, lane 4). A mutant leucine-zipper motif (KZiP) replacement was incapable of rescuing the ΔNC assembly defect (Fig. 6A, lane 5), but in spite of producing a wt-comparable level of VLPs, ΔNC(wtZiP) did not package hA3G as efficiently as wt (lane 4 vs. lane 2).

We also examined whether human coronavirus 229E (HCoV-229E) N protein (having approximately 30% homology with SARS-CoV N at the amino acid level) (Tswen-Kei Tang, 2005) is capable of conferring the ability to package hA3G when substituted for HIV-1 NC. To perform this test, we constructed NC(229EN2) (an NC[N2] counterpart) by inserting the HCoV-229E carboxyl-terminal half nucleocapsid coding sequence into the deleted HIV-1 NC region. The resulting construct was transiently co-expressed with hA3G in 293T cells. The results indicate that NC(229EN2) can also package hA3G to a degree comparable to that of wt when released VLPs are at a similar level (data not shown). To mitigate the impact of overexpressed hA3G on this conclusion, we repeated the experiment by co-expressing hA3G with wt or the chimeric construct in 293 cells. As the results in Fig. 6B indicate, the carboxyl-terminal half of HCoV-229E N (which also contains a putative self-association domain) (Tswen-Kei Tang, 2005) was capable of replacing the HIV-1 NC function with respect to VLP assembly and hA3G packaging—that is, substantial amounts of VLPs and hA3G were detected in NC(229EN2) transfectant supernatant (lane 4). To determine whether the interaction between hA3G and HCoV-229E N also requires RNA, we performed a GST pull-down assay in the presence or absence of RNase. As expected, the GST fusions containing the full-length (GST-229EN), amino-terminal half (GST-229EN1), or carboxyl-terminal half (GST-229EN2) of the HCoV-229E N sequence were capable of efficient hA3G pull-down, which is also dependent on the presence of RNA (Fig. 7). These data suggest that HCoV-229E N and SARS-CoV N may share a propensity for hA3G-association.

Discussion

Any conclusion that SARS-CoV N enables efficient hA3G packaging into VLPs when substituted for HIV-1 NC must be tempered when over-expression systems are considered. Still, the evidence presented in this paper suggests an association between SARS-CoV N and hA3G—that is, the leucine-zipper domain is incapable of conferring the ability to package hA3G when substituted for HIV-1 NC even though it enables efficient VLP production. Moreover, assembly-competent chimeras with various SARS-CoV N protein sequences inserted into the deleted HIV-1 NC did not have equal hA3G packaging capabilities: NC(N2) and NC(N4) exhibited a higher level of VLP-associated hA3G than NC(N1). Results from a GST pull-down assay suggest that the SARS-CoV N domain associated with hA3G is largely contained within the central N region between residues 86 and 302 (Fig. 3). Although GST-N1 and GST-N6 can pull down hA3G, we found that NC(N1) and NC(N6) are incapable of packaging hA3G as efficiently as wt or NC (N2). Therefore, insufficient hA3G incorporation into NC(N1) and NC (N6) may be due in part to steric hindrance in a chimeric protein context.

Evidence that a carboxyl-terminal self-association domain of SARS-CoV N or HCoV-229E N (as opposed to the amino-terminal RNA-binding domain) confers the ability to efficiently package hA3G suggests that for this specific purpose, HIV-1 NC can be replaced by a protein sequence that does not encapsidate HIV-1 genomic RNA. Given the number of studies demonstrating that viral genomic RNA is dispensable for efficient A3G packaging (Alce and Popik, 2004; Cen et al., 2004; Khan et al., 2005; Luo et al., 2004; Navarro et al., 2005; Schafer et al., 2004; Svarovskaia et al., 2004; Zennou et al., 2004), any genomic RNA packaging defect that does exist should not exert a significant impact on the hA3G package. The finding that efficient SARS-CoV N association with hA3G is RNA-dependent (Fig. 3) agrees with the proposal that RNA (viral or nonspecific) is required for mediating hA3G–Gag association and hA3G incorporation into virions (Svarovskaia et al., 2004; Zennou et al., 2004). We assumed that the chimeras considered competent in hA3G packaging are capable of packaging considerable amounts of RNA, since the SARS-CoV N (Hsieh et al., 2005; Luo et al., 2006) and HIV-1 MA domains (Burniston et al., 1999; Ott et al., 2005) both possess nucleic acid binding properties that may confer RNA packaging ability. Using a RNA quantification assay as described by Chang et al. (2008), we found that NC(N2) VLPs contain RNA at approximately 80% of the level measured in HIV-1 Gag VLPs (data not shown).

Recent studies have suggested that hA3G preferentially binds with cellular 7SL RNA, which in turn facilitates an association between RNA-bound hA3G and NC for viral incorporation (Bogerd and Cullen, 2008; Wang et al., 2007). Accordingly, 7SL RNA apparently plays a key role in determining hA3G packaging into HIV-1 virions. Additional experiments are required to determine whether SARS-CoV or NC(N2) are as capable as HIV-1 in terms of packaging 7SL RNA. To date, one *in vitro* study has demonstrated that A3G binds to RNA prior to HIV-1 NC association (Bogerd and Cullen, 2008). Accordingly, it may be that the interactions required for A3G/RNA/NC ternary complex formation involve specific contacts between NC and both A3G and A3G-bound RNA. SARS-CoV N association with hA3G may in large part depend on N binding to hA3G-bound RNA, since the SARS-CoV N contains clusters of basic residues in the amino- and carboxyl-terminal regions that may confer RNA-binding ability (Hsieh et al., 2005). Extensive genetic analyses indicate that SARS-CoV N RNA-binding domains are largely located between amino acid residues 45–181 (Huang et al., 2004a), 248–280 (Chen et al., 2007a; Luo et al., 2006), and 363–382

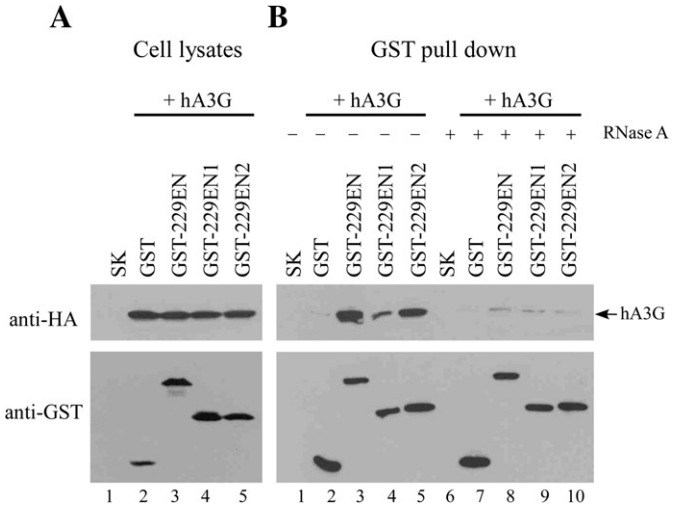

Fig. 7. Association of HCoV-229E nucleocapsid protein with hA3G. (A) 293T cells were co-transfected with a human A3G (hA3G) expression vector and pBlueScript SK, GST, or GST fusions encoding the full-length (GST-229EN), amino-terminal (GST-229EN1) or carboxyl-terminal (GST-229EN2) half of HCoV-229E nucleocapsid protein. Cell lysates were subjected to Western immunoblotting 48 h post-transfection. (B) Equal amounts of cell lysates were treated with (lanes 6–10) or without (lanes 1–5) 0.2 mg/ml DNase-free RNase A, followed by GST pull-down assay as described in the legend of Fig. 3.

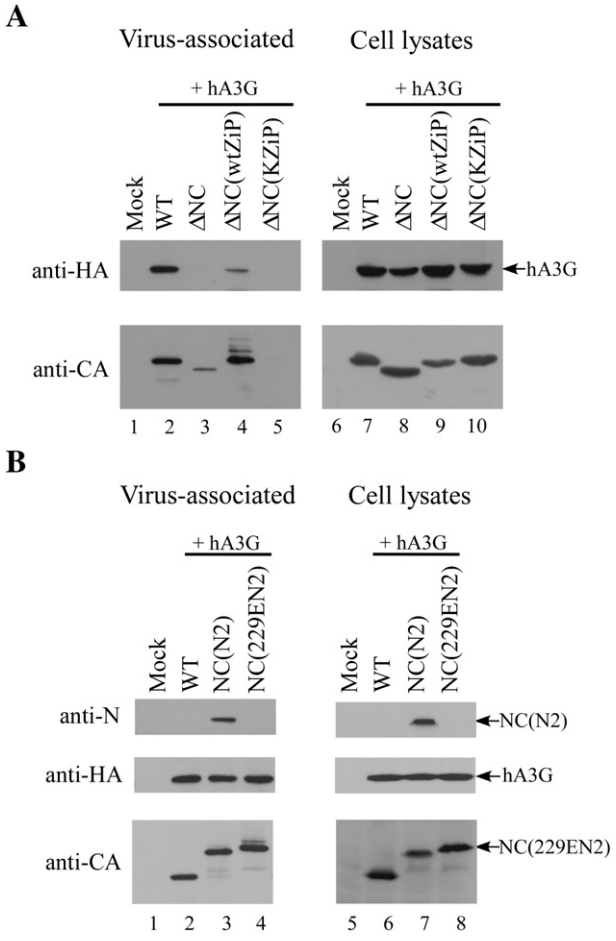

Fig. 6. Incorporation of hA3G into chimeric VLPs. 293T (panel A) or 293 (panel B) cells were co-transfected with a human APOBEC3G (hA3G) expression vector and indicated plasmid. ΔNC(wtZiP) and ΔNC(KZiP) contained HIV-1 NC replacements consisting of wild-type or a mutated version of a leucine-zipper domain, respectively. NC(229EN2) contained the carboxyl-terminal half of a 229E human coronavirus nucleocapsid as a replacement for HIV-1 NC. At 48–72 h or 72 h (panel B) post-transfection, cells and supernatant were collected and subjected to Western immunoblotting. Wild-type Gag and chimeric proteins were probed with a monoclonal antibody directed against HIV-1 CA or SARS-CoV N; an anti-HA monoclonal antibody was used to detect hA3G.

(Luo et al., 2006), all of which contain large quantities of basic residues. It is conceivable that basic residue clusters within SARS-CoV N make a significant contribution to hA3G–N association by enhancing N binding to hA3G-associated RNA. Compatible with this hypothesis, we found that the GST fusions GST-CoN, GST-N1, GST-N2 and GST-N6, all of which contain most of the residues involved in RNA-binding, are competent in their associations with hA3G (Fig. 3). The exception to this rule is GST-N5, which is unable to pull down hA3G despite bearing a putative RNA-binding domain (residues 363–382). Our finding that the essential region for hA3G packaging into HIV-1 or SARS-CoV VLPs resides between codons 104 and 156 is compatible with a genetic analysis demonstrating that residues 124 to 127 are responsible for hA3G viral incorporation (Huthoff and Malim, 2007).

A very recent study suggests that hA3G contains a necessary and sufficient cytoplasmic retention signal located between residues 113 and 128 (Bennett et al., 2008). Consistent with this report, our immunofluorescence experiment results indicate that cells expressing the hA3G deletion mutant Δ1–156 show fluorescence staining in both the nucleus and cytoplasm; in contrast, fluorescence in cells expressing wt or hA3G mutants Δ1–104, Δ157–384, or Δ246–384 is predominantly present in cell cytoplasm (data not shown). However, the mislocalization of Δ1–156 does not account for its defective incorporation into HIV-1 or SARS-CoV VLPs, since GST pull-down assay results suggest that cytoplasmic hA3G(Δ1–156) is still incapable of associating with SARS-CoV N (data not shown).

HCoV-229E N and SARS-CoV N share two conserved sequences: one from residues 50 to 170 and the other from 250 to 360 (Tswen-Kei Tang, 2005). Combined, the ability of NC(229EN2) to package hA3G and the RNA-dependent association of HCoV-229E N with hA3G (Fig. 7) imply that in addition to SARS-CoV N, coronaviral N products may associate with hA3G via binding with RNA. However, human T-cell leukemia virus type 1 (HTLV-1) has been found to prevent hA3G packaging through Gag NC domain action (Derse et al., 2007), suggesting that some RNA viruses are incapable of packaging A3G. Our results indicate that the presence of the hA3G first linker region is required for hA3G to be packaged into either HIV-1 Gag or SARS-CoV VLPs. It is possible that an RNA/hA3G complex, either alone or in combination with other cellular factors, is an acceptable structure for an association between HIV-1 NC and SARS-CoV N.

Here we demonstrated for the first time that SARS-CoV is capable of packaging hA3G via the SARS-CoV N protein. It remains to be determined whether chimeric NC(N2) or SARS-CoV can package endogenous A3G as efficiently as HIV-1. The biological significance of a SARS-CoV N association with hA3G also requires further exploration. According to one report, hA3G is capable of editing virus-associated HIV-1 RNA (Bishop et al., 2004); the hA3G-mediated inhibition of viral replication may be independent of its cytidine deaminase activity (Rösler et al., 2005; Turelli et al., 2004). Since humans are not natural hosts for SARS-CoV (Li et al., 2005), human susceptibility implies that cells infected by SARS-CoV may not express A3G, or SARS-CoV may have evolved to counteract A3G anti-viral activity. Further studies are required to address this issue.

Materials and methods

Plasmid construction

The parental HIV-1 proviral plasmid DNA used in this study was HXB_2 (Ratner et al., 1985). The cDNA clone of the SARS-CoV N (SARS coronavirus strain TWC, GenBank accession number AY321118) was provided by the Centers for Disease Control of the Department of Health, Taiwan. HIV-1 NC-deletion mutants ΔNC, delNC, and ΔPC and chimeras ΔNC(CoN), NC(CoN), NC(N1), NC(N2), NC(N3), NC(N4), NC(N5), NC(N6), NC(N7), ΔNC(wtZiP) and ΔNC(KZiP) were all as previously described (Wang et al., 2008). Primers used for making NC(229EN2) were 5′-CGCAATCGATTCATGAAGGCAGTTGCT-3′ (forward) and 5′-CTTCGGATCCCGTTTACTTCATCAAT-3′ (reverse) using a coronavirus 229E (HCoV-229E) nucleocapsid expression vector pTRE-HN (Schelle et al., 2005) as template (kindly provided by Volker Thiel). To construct a Vif-deficient (ΔVif) mutation, Vif-encoding plasmid DNA was digested with NdeI, filled in, and relegated, resulting in a shift in the Vif open reading frame. All of the engineered constructs were cloned into the PR-defective HIV-1 proviral expression vector HIVgptD25 (Wang et al., 2000). Human APOBEC3G (hA3G) expression vector pcDNA3.1-APOBEC3G-HA (Sheehy et al., 2002; Stopak et al., 2003) was obtained through the NIH AIDS Research and Reference Reagent Program. hA3G deletion mutants were gifts from S. Cen (Cen et al., 2004). Mammalian expression vectors encoding SARS-CoV M and N were provided by G.J. Nabel (Huang et al., 2004b).

To construct GST fusions, amplicons containing SARS-CoV N or HCoV-229E N coding sequences were digested with BamHI and ClaI and fused to the C-terminus of GST, which is directed by a mammalian elongation factor 1a promoter (Cortes et al., 1996). Primers for cloning GST fusions were GST-CoN, 5′-TAAAGGATCCTCTGATAATGGACCC-3′ (forward), 5′-TCATATCGATTTATGCCTGAGTTGAATC-3′ (reverse); GST-N1, 5′-TAAAGGATCCTCTGATAATGGACCC-3′ (forward), 5′-GCTCATCGATTAGCTAGCCATTCGAGC-3′ (reverse); GST-N2, 5′-TGGCTGGATCCGGTGGTGAAACTGCC-3′ (forward), 5′-TCATATCGATTTATGCCTGAGTTGAATC-3′ (reverse); GST-N5, 5′-ATTACGGATCCTGGCCGCAAATTGCA-3′ (forward), 5′-TCATATCGATTTATGCCTGAGTTGAATC-3′ (reverse); GST-N6, 5′-TAAAGGATCCTCTGATAATGGACCC-3′ (forward), 5′-GCTCATCGATTATGTTGTTCCTTGAGG-3′(reverse); GST-N7, 5′-TAAAGGATCCTCTGATAATGGACCC-3′ (forward), 5′-GCTCATCGATTAGCCAATTTGGTCAT-3′ (reverse); GST-229EN, 5′-CGGGATCCGCTACAGTCAAATGG-3′ (forward), 5′-CCATCGATTAGTTTACTTCATCAAT-3′ (reverse); GST-229EN1, 5′-CGGGATCCGCTACAGTCAAATGG-3′ (forward), 5′-CCATCGATTATTCCTGAGGCTTGTC-3′ (reverse); and GST-229EN2, 5′-CGGGATCCATGAAGGCAGTTGCT-3′ (forward), 5′-CCATCGATTAGTTTACTTCATCAAT-3′ (reverse). Mutations were confirmed by restriction enzyme digestion or DNA sequencing.

Cell culture and transfection

293T and 293 cells were maintained in Dulbecco's modified Eagle's medium (DMEM) supplemented with 10% fetal calf serum (GIBCO). Confluent 293T or 293 cells were trypsinized and split 1:10 onto 10-cm dishes 24 h prior to transfection. For each construct, cells were transfected with 20 μg of plasmid DNA using the calcium phosphate precipitation method; 50 μm chloroquine was added to enhance transfection efficiency. Unless otherwise indicated, 10 μg of each plasmid was used for co-transfection. Culture supernatant and cells were harvested for protein analysis 2–3 d post-transfection.

Western immunoblot

At 48–72 h post-transfection, supernatant from transfected 293T or 293 cells was collected, filtered, and centrifuged through 2 ml of 20% sucrose in TSE (10 mM Tris–HCl [pH 7.5], 100 mM NaCl, 1 mM EDTA plus 0.1 mM phenylmethylsulfonyl fluoride [PMSF]) at 4 °C for 40 min at 274,000 ×*g*. Pellets were suspended in IPB (20 mM Tris–HCl [pH 7.5], 150 mM NaCl, 1 mM EDTA, 0.1% SDS, 0.5% sodium deoxycholate, 1% Triton X-100, 0.02% sodium azide) plus 0.1 mM PMSF. Next, cells were rinsed with ice-cold phosphate-buffered saline (PBS), collected in IPB plus 0.1 mM PMSF, and microcentrifuged at 4 °C for 15 min at 13,700 ×*g* to remove cell debris. Supernatant and cell samples were mixed with equal volumes of 2X sample buffer (12.5 mM Tris–HCl [pH 6.8], 2% SDS, 20% glycerol, 0.25% bromophenol blue) and 5% β-mercaptoethanol and boiled for 5 min. Samples were resolved by electrophoresis on SDS-polyacrylamide gels and electroblotted onto nitrocellulose membranes. Membrane-bound Gag or chimeric proteins were immunodetected using a mouse monoclonal antibody directed against HIV-1 p24CA (Wang et al., 1998) or the

SARS-CoV nucleocapsid (Wang et al., 2008). SARS-CoV M was detected with a rabbit anti-M polyclonal antibody (Rockland). HA-tagged hA3G was probed with a mouse anti-HA (Sigma) monoclonal antibody at a dilution of 1:5000. For HIV-1 Vif detection, a rabbit anti-Vif polyclonal antibody (Goncalves et al., 1994) was used at a 1:2000 dilution. The secondary antibody was a sheep anti-mouse or donkey anti-rabbit horseradish peroxidase-(HRP) conjugated antibody (Invitrogen), both at 1:5000 dilutions. To detect GST and GST fusions, anti-GST HRP conjugate (Amersham) was used at a 1:5000 dilution. Horseradish peroxidase activity was detected according to the manufacturer's protocol.

GST pull-down assay

293T cells either mock transfected or transfected with GST fusion expression vectors were collected, lysed in RIPA buffer (140 mM NaCl, 8 mM Na_2HPO_4, 2 mM NaH_2PO_4, 1% NP-40, 0.5% sodium deoxycholate, 0.05% SDS) containing complete protease inhibitor cocktail (Roche), and microcentrifuged at 4 °C for 15 min at 13,700 ×*g* (14,000 rpm) to remove cell debris. Aliquots of post-nuclear supernatant (PNS) were mixed with equal amounts of 2× sample buffer and 5% β-mercaptoethanol and held for Western blot analysis. RIPA buffer was added to the remaining PNS samples to final volumes of 500 μl. Each sample was mixed with glutathione-agarose beads (30 μl) (Sigma) and rocked for 2 h at 4 °C. Bead-bound complexes were pelleted, washed tree times with RIPA buffer, twice with PBS, eluted at 1× sample buffer with 5% β-mercaptoethanol, boiled for 5 min, and subjected to SDS-10% PAGE as described above.

Sucrose density gradient fractionation

Supernatant cultures of transfected 293T cells were collected, filtered, and centrifuged through 2 ml 20% sucrose cushions as described above. Viral pellets were suspended in PBS buffer and laid on top of a pre-made 20–60% sucrose gradient consisting of 1 ml layers of 20, 30, 40, 50 and 60% sucrose in TSE that had been allowed to sit for 2 h. Gradients were centrifuged in an SW50.1 rotor at 40,000 rpm (274,000 ×*g*) for 16 h at 4 °C; 500 μl fractions were collected from top to bottom. Sucrose density was measured for each fraction. Proteins in each fraction were precipitated with 10% trichloroacetic acid (TCA) and subjected to Western immunoblotting.

Laser scanning immunofluorescence microscopy

Confluent 293 cells were split 1:80 onto coverslips 24 h before transfection. Two days post-transfection, cells were fixed at 4 °C for 20 min with ice-cold PBS containing 3.7% formaldehyde, washed once with PBS and once with DMEM plus 10% heat-inactivated calf serum (DMEM/calf serum), and permeabilized at room temperature for 10 min in PBS plus 0.2% Triton X-100. Samples were incubated with the primary antibody for 1 h and secondary antibody for 30 min. Following each incubation, samples were subjected to three washes (5 to 10 min each) with DMEM/calf serum. The primary antibody was an anti-HA (Sigma) at a 1:200 dilution. A rabbit anti-mouse rhodamine-conjugated antibody at a 1:100 dilution served as the secondary antibody (Cappel, ICN Pharmaceuticals, Aurora, Ohio, USA). After the final DMEM/calf serum wash, the coverslips were washed three times with PBS and mounted in 50% glycerol in PBS for viewing. Images were taken using an epifluorescence microscope (Olympus AX-80) or laser scanning confocal microscope (Olympus FV300).

Acknowledgments

We thank Y.-P. Li for the reagents and technical assistance, Cen Shan for providing the hA3G deletion mutant plasmids, Volker Thiel for the HCoV-229E N cDNA, and G. Nabel for the SARS-CoV M and N expression vectors. The following reagents were obtained through the NIH AIDS Research and Reference Reagent Program: pcDNA3.1-APOBEC3G-HA from Warner C. Greene and HIV-1 Vif antiserum from D. Gabuzda. This work was supported by grants VGH94-314 from the Taipei Veterans General Hospital and NSC94-2320-B-010-035 from the National Science Council, Taiwan, Republic of China.

References

Accola, M.A., Strack, B., Gottlinger, H.G., 2000. Efficient particle production by minimal gag constructs which retain the carboxy-terminal domain of human immunodeficiency virus type 1 capsid-p2 and a late assembly domain. J. Virol. 74 (12), 5395–5402.

Alce, T.M., Popik, W., 2004. APOBEC3G is incorporated into virus-like particles by a direct interaction with HIV-1 Gag nucleocapsid protein. J. Biol. Chem. 279 (33), 34083–34086.

Bennett, R.P., Nelle, T.D., Wills, J.W., 1993. Functional chimeras of the *Rous sarcoma virus* and human immunodeficiency virus gag proteins. J. Virol. 67 (11), 6487–6498.

Bennett, R.P., Presnyak, V., Wedekind, J.E., Smith, H.C., 2008. Nuclear exclusion of the HIV-1 host defense factor APOBEC3G requires a novel cytoplasmic retention signal and is not dependent on RNA binding. J. Biol. Chem. 283 (12), 7320–7327.

Berkowitz, R.D., Luban, J., Goff, S.P., 1993. Specific binding of human immunodeficiency virus type 1 gag polyprotein and nucleocapsid protein to viral RNAs detected by RNA mobility shift assays. J. Virol. 67 (12), 7190–7200.

Berkowitz, R.D., Ohagen, A., Hoglund, S., Goff, S.P., 1995. Retroviral nucleocapsid domains mediate the specific recognition of genomic viral RNAs by chimeric Gag polyproteins during RNA packaging in vivo. J. Virol. 69 (10), 6445–6456.

Bishop, K.N., Holmes, R.K., Sheehy, A.M., Malim, M.H., 2004. APOBEC-mediated editing of viral RNA. Science 305 (5684), 645.

Bogerd, H.P., Cullen, B.R., 2008. Single-stranded RNA facilitates nucleocapsid: APOBEC3G complex formation. RNA 14 (6), 1228–1236.

Bowzard, J.B., Bennett, R.P., Krishna, N.K., Ernst, S.M., Rein, A., Wills, J.W., 1998. Importance of basic residues in the nucleocapsid sequence for retrovirus Gag assembly and complementation rescue. J. Virol. 72 (11), 9034–9044.

Burniston, M.T., Cimarelli, A., Colgan, J., Curtis, S.P., Luban, J., 1999. Human immunodeficiency virus type 1 Gag polyprotein multimerization requires the nucleocapsid domain and RNA and is promoted by the capsid-dimer interface and the basic region of matrix protein. J. Virol. 73 (10), 8527–8540.

Cen, S., Guo, F., Niu, M., Saadatmand, J., Deflassieux, J., Kleiman, L., 2004. The interaction between HIV-1 Gag and APOBEC3G. J. Biol. Chem. 279 (32), 33177–33184.

Chang, C.-Y., Chang, Y.-F., Wang, S.-M., Tseng, Y.-T., Huang, K.-J., Wang, C.-T., 2008. HIV-1 matrix protein repositioning in nucleocapsid region fails to confer virus-like particle assembly. Virology 378 (1), 97–104.

Chen, C.Y., Chang, C.K., Chang, Y.W., Sue, S.C., Bai, H.I., Riang, L., Hsiao, C.D., Huang, T.H., 2007a. Structure of the SARS coronavirus nucleocapsid protein RNA-binding dimerization domain suggests a mechanism for helical packaging of viral RNA. J. Mol. Biol. 368 (4), 1075–1086.

Chen, K.-M., Martemyanova, N., Lu, Y., Shindo, K., Matsuo, H., Harris, R.S., 2007b. Extensive mutagenesis experiments corroborate a structural model for the DNA deaminase domain of APOBEC3G. FEBS Lett. 581 (24), 4761–4766.

Conticello, S.G., Harris, R.S., Neuberger, M.S., 2003. The Vif protein of HIV triggers degradation of the human antiretroviral DNA deaminase APOBEC3G. Curr. Biol. 13 (22), 2009–2013.

Cortes, P., Weis-Garcia, F., Misulovin, Z., Nussenzweig, A., Lai, J. -S., Li, G., Nussenzweig, M., Baltimore, D., 1996. In vitro V(D)J recombination: signal joint formation. PNAS 93 (24), 14008–14013.

Cullen, B.R., 2006. Role and mechanism of action of the APOBEC3 family of antiretroviral resistance factors. J. Virol. 80 (3), 1067–1076.

Derse, D., Hill, S.A., Princler, G., Lloyd, P., Heidecker, G., 2007. Resistance of human T cell leukemia virus type 1 to APOBEC3G restriction is mediated by elements in nucleocapsid. Proc. Natl. Acad. Sci. 104 (8), 2915–2920.

Goncalves, J., Jallepalli, P., Gabuzda, D.H., 1994. Subcellular localization of the Vif protein of human immunodeficiency virus type 1. J. Virol. 68 (2), 704–712.

Harris, R.S., Bishop, K.N., Sheehy, A.M., Craig, H.M., Petersen-Mahrt, S.K., Watt, I.N., Neuberger, M.S., Malim, M.H., 2003. DNA deamination mediates innate immunity to retroviral infection. Cell 113 (6), 803–809.

He, R., Dobie, F., Ballantine, M., Leeson, A., Li, Y., Bastien, N., Cutts, T., Andonov, A., Cao, J., Booth, T.F., 2004. Analysis of multimerization of the SARS coronavirus nucleocapsid protein. Biochem. Biophys. Res. Commun. 316 (2), 476–483.

Hsieh, P.-K., Chang, S.C., Huang, C.-C., Lee, T.-T., Hsiao, C.-W., Kou, Y.-H., Chen, I.Y., Chang, C.-K., Huang, T.-H., Chang, M.-F., 2005. Assembly of severe acute respiratory syndrome coronavirus RNA packaging signal into virus-like particles is nucleocapsid dependent. J. Virol. 79 (22), 13848–13855.

Huang, Q., Yu, L., Petros, A.M., Gunasekera, A., Liu, Z., Xu, N., Hajduk, P., Mack, J., Fesik, S.W., Olejniczak, E.T., 2004a. Structure of the N-terminal RNA-binding domain of the SARS CoV nucleocapsid protein. Biochemistry 43 (20), 6059–6063.

Huang, Y., Yang, Z.Y., Kong, W.P., Nabel, G.J., 2004b. Generation of synthetic severe acute respiratory syndrome coronavirus pseudoparticles: implications for assembly and vaccine production. J. Virol. 78 (22), 12557–12565.

Huthoff, H., Malim, M.H., 2007. Identification of amino acid residues in APOBEC3G required for regulation by human immunodeficiency virus type 1 Vif and virion encapsidation. J. Virol. 81 (8), 3807–3815.

Johnson, M.C., Scobie, H.M., Ma, Y.M., Vogt, V.M., 2002. Nucleic acid-independent retrovirus assembly can be driven by dimerization. J. Virol. 76 (22), 11177–11185.
Kao, S., Khan, M.A., Miyagi, E., Plishka, R., Buckler-White, A., Strebel, K., 2003. The human immunodeficiency virus type 1 Vif protein reduces intracellular expression and inhibits packaging of APOBEC3G (CEM15), a cellular inhibitor of virus infectivity. J. Virol. 77 (21), 11398–11407.
Khan, M.A., Kao, S., Miyagi, E., Takeuchi, H., Goila-Gaur, R., Opi, S., Gipson, C.L., Parslow, T.G., Ly, H., Strebel, K., 2005. Viral RNA is required for the association of APOBEC3G with human immunodeficiency virus type 1 nucleoprotein complexes. J. Virol. 79 (9), 5870–5874.
Li, W., Shi, Z., Yu, M., Ren, W., Smith, C., Epstein, J.H., Wang, H., Crameri, G., Hu, Z., Zhang, H., Zhang, J., McEachern, J., Field, H., Daszak, P., Eaton, B.T., Zhang, S., Wang, L.-F., 2005. Bats are natural reservoirs of SARS-Like coronaviruses. Science 310 (5748), 676–679.
Liu, B., Yu, X., Luo, K., Yu, Y., Yu, X.-F., 2004. Influence of primate lentiviral Vif and proteasome inhibitors on human immunodeficiency virus type 1 virion packaging of APOBEC3G. J. Virol. 78 (4), 2072–2081.
Luo, K., Liu, B., Xiao, Z., Yu, Y., Yu, X., Gorelick, R., Yu, X.-F., 2004. Amino-terminal region of the human immunodeficiency virus type 1 nucleocapsid is required for human APOBEC3G packaging. J. Virol. 78 (21), 11841–11852.
Luo, H., Chen, J., Chen, K., Shen, X., Jiang, H., 2006. Carboxyl terminus of severe acute respiratory syndrome coronavirus nucleocapsid protein: self-association analysis and nucleic acid binding characterization. Biochemistry 45 (39), 11827–11835.
Mangeat, B., Turelli, P., Caron, G., Friedli, M., Perrin, L., Trono, D., 2003. Broad antiretroviral defence by human APOBEC3G through lethal editing of nascent reverse transcripts. Nature 424 (6944), 99–103.
Mariani, R., Chen, D., Schrofelbauer, B., Navarro, F., Konig, R., Bollman, B., Munk, C., Nymark-McMahon, H., Landau, N.R., 2003. Species-specific exclusion of APOBEC3G from HIV-1 virions by Vif. Cell 114 (1), 21–31.
Marin, M., Rose, K.M., Kozak, S.L., Kabat, D., 2003. HIV-1 Vif protein binds the editing enzyme APOBEC3G and induces its degradation. Nat. Med. 9 (11), 1398–1403.
Mehle, A., Strack, B., Ancuta, P., Zhang, C., McPike, M., Gabuzda, D., 2004. Vif overcomes the innate antiviral activity of APOBEC3G by promoting its degradation in the ubiquitin–proteasome pathway. J. Biol. Chem. 279 (9), 7792–7798.
Narayanan, K., Kim, K.H., Makino, S., 2003. Characterization of N protein self-association in coronavirus ribonucleoprotein complexes. Virus Res. 98 (2), 131–140.
Navarro, F., Bollman, B., Chen, H., Konig, R., Yu, Q., Chiles, K., Landau, N.R., 2005. Complementary function of the two catalytic domains of APOBEC3G. Virology 333 (2), 374–386.
Ott, D.E., Coren, L.V., Gagliardi, T.D., 2005. Redundant roles for nucleocapsid and matrix RNA-binding sequences in human immunodeficiency virus type 1 assembly. J. Virol. 79 (22), 13839–13847.
Poon, D.T., Wu, J., Aldovini, A., 1996. Charged amino acid residues of human immunodeficiency virus type 1 nucleocapsid p7 protein involved in RNA packaging and infectivity. J. Virol. 70 (10), 6607–6616.
Rösler, C., Köck, J., Kann, M., Malim, M.H., Blum, H.E., Baumert, T.F., Weizsäcker, F.V., 2005. APOBEC-mediated interference with hepadnavirus production. HEPATOLOGY 42, 301–309.
Ratner, L., Haseltine, W., Patarca, R., Livak, K.J., Starcich, B., Josephs, S.F., Doran, E.R., Rafalski, J.A., Whitehorn, E.A., Baumeister, K., et al., 1985. Complete nucleotide sequence of the AIDS virus, HTLV-III. Nature 313 (6000), 277–284.
Schafer, A., Bogerd, H.P., Cullen, B.R., 2004. Specific packaging of APOBEC3G into HIV-1 virions is mediated by the nucleocapsid domain of the gag polyprotein precursor. Virology 328 (2), 163–168.
Schelle, B., Karl, N., Ludewig, B., Siddell, S.G., Thiel, V., 2005. Selective replication of coronavirus genomes that express nucleocapsid protein. J. Virol. 79 (11), 6620–6630.
Sheehy, A.M., Gaddis, N.C., Choi, J.D., Malim, M.H., 2002. Isolation of a human gene that inhibits HIV-1 infection and is suppressed by the viral Vif protein. Nature 418 (6898), 646–650.
Sheehy, A.M., Gaddis, N.C., Malim, M.H., 2003. The antiretroviral enzyme APOBEC3G is degraded by the proteasome in response to HIV-1 Vif. Nat. Med. 9 (11), 1404–1407.
Stopak, K., de Noronha, C., Yonemoto, W., Greene, W.C., 2003. HIV-1 Vif blocks the antiviral activity of APOBEC3G by impairing both its translation and intracellular stability. Mol. Cell 12 (3), 591–601.
Surjit, M., Liu, B., Kumar, P., Chow, V.T., Lal, S.K., 2004. The nucleocapsid protein of the SARS coronavirus is capable of self-association through a C-terminal 209 amino acid interaction domain. Biochem. Biophys. Res. Commun. 317 (4), 1030–1036.
Svarovskaia, E.S., Xu, H., Mbisa, J.L., Barr, R., Gorelick, R.J., Ono, A., Freed, E.O., Hu, W.-S., Pathak, V.K., 2004. Human apolipoprotein B mRNA-editing enzyme-catalytic polypeptide-like 3G (APOBEC3G) is incorporated into HIV-1 virions through interactions with viral and nonviral RNAs. J. Biol. Chem. 279 (34), 35822–35828.
Tswen-Kei Tang, W., M.P.J., C., S.-T., H., M.-H., H., M.-H., P., F.-M., Y., H.-M., C., J.-H., Y., C.-W., W., A.H., 2005. Biochemical and immunological studies of nucleocapsid proteins of severe acute respiratory syndrome and 229E human coronaviruses. PROTEOMICS 5 (4), 925–937.
Turelli, P., Mangeat, B., Jost, S., Vianin, S., Trono, D., 2004. Inhibition of hepatitis B virus replication by APOBEC3G. Science 303 (5665), 1829.
Wang, C.-T., Lai, H.-Y., Li, J.-J., 1998. Analysis of minimal human immunodeficiency virus type 1 Gag coding sequences capable of virus-like particle assembly and release. J. Virol. 72 (10), 7950–7959.
Wang, C.-T., Chou, Y.-C., Chiang, C.-C., 2000. Assembly and processing of human immunodeficiency virus Gag mutants containing a partial replacement of the matrix domain by the viral protease domain. J. Virol. 74 (7), 3418–3422.
Wang, T., Tian, C., Zhang, W., Luo, K., Sarkis, P.T.N., Yu, L., Liu, B., Yu, Y., Yu, X.-F., 2007. 7SL RNA mediates virion packaging of the antiviral cytidine deaminase APOBEC3G. J. Virol. 81 (23), 13112–13124.
Wang, S.-M., Chang, Y.-F., Chen, Y.-M., Wang, C.-T., 2008. Severe acute respiratory syndrome coronavirus nucleocapsid protein confers ability to efficiently produce virus-like particles when substituted for the human immunodeficiency virus nucleocapsid domain. J. Biomed. Sci. 15 (6), 719–729.
Yu, X., Yu, Y., Liu, B., Luo, K., Kong, W., Mao, P., Yu, X. -F., 2003. Induction of APOBEC3G ubiquitination and degradation by an HIV-1 Vif-Cul5-SCF complex. Science 302 (5647), 1056–1060.
Yu, Q., Konig, R., Pillai, S., Chiles, K., Kearney, M., Palmer, S., Richman, D., Coffin, J.M., Landau, N.R., 2004. Single-strand specificity of APOBEC3G accounts for minus-strand deamination of the HIV genome. Nat. Struct. Mol. Biol. 11 (5), 435–442.
Yu, I.M., Gustafson, C.L., Diao, J., Burgner 2nd, J.W., Li, Z., Zhang, J., Chen, J., 2005. Recombinant severe acute respiratory syndrome (SARS) coronavirus nucleocapsid protein forms a dimer through its C-terminal domain. J. Biol. Chem. 280 (24), 23280–23286.
Zennou, V., Perez-Caballero, D., Gottlinger, H., Bieniasz, P.D., 2004. APOBEC3G incorporation into human immunodeficiency virus type 1 particles. J. Virol. 78 (21), 12058–12061.
Zhang, Y., Barklis, E., 1997. Effects of nucleocapsid mutations on human immunodeficiency virus assembly and RNA encapsidation. J. Virol. 71 (9), 6765–6776.
Zhang, Y., Qian, H., Love, Z., Barklis, E., 1998. Analysis of the assembly function of the human immunodeficiency virus type 1 Gag protein nucleocapsid domain. J. Virol. 72 (3), 1782–1789.
Zhang, H., Yang, B., Pomerantz, R.J., Zhang, C., Arunachalam, S.C., Gao, L., 2003. The cytidine deaminase CEM15 induces hypermutation in newly synthesized HIV-1 DNA. Nature 424 (6944), 94–98.